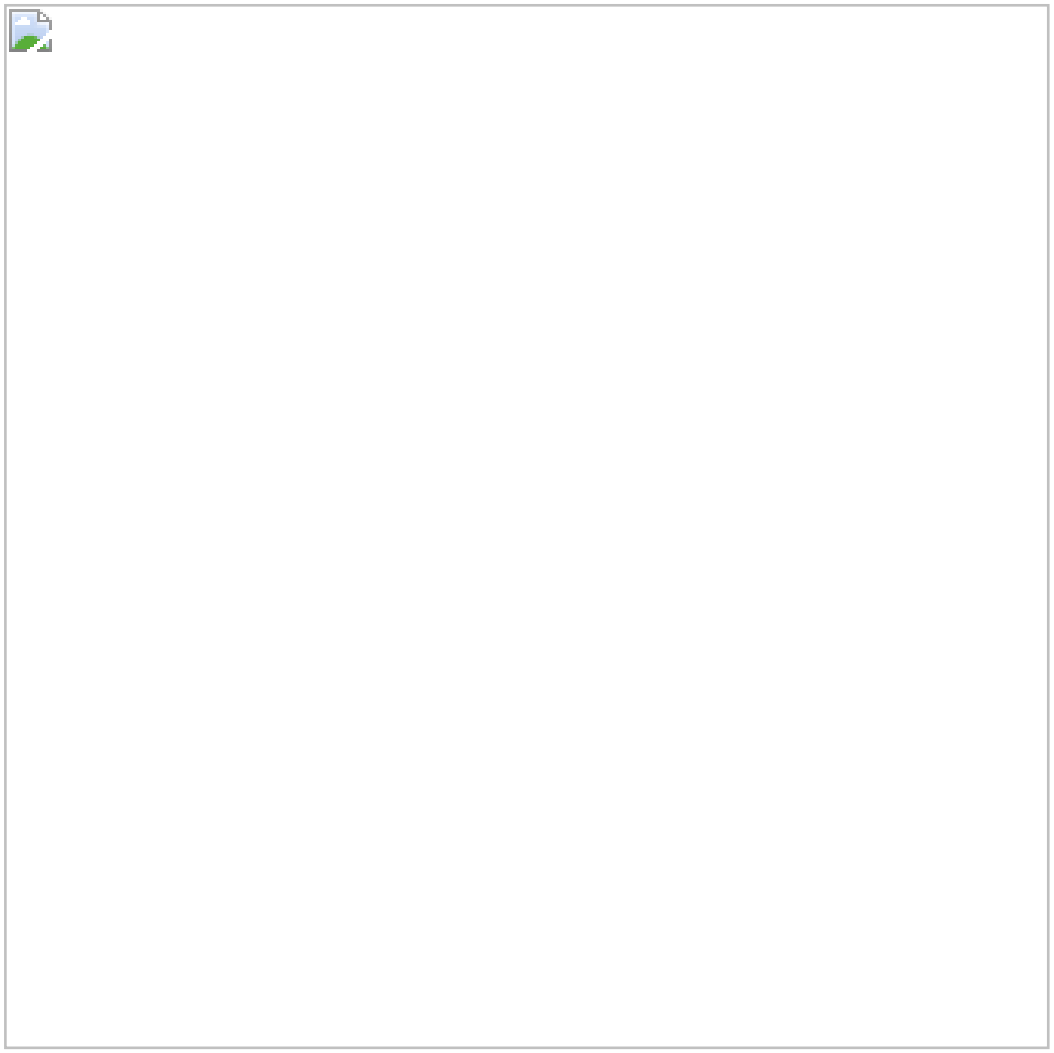

Hydrological Components and Sediment Yield Response to Land Use Land Cover Change in The Ajora-Woybo Watershed of Omo-Gibe Basin, Ethiopia

Authors: Toma, Meseret Bekele, Belete, Mulugeta Dadi, and Ulsido, Mihret Dananto

Source: Air, Soil and Water Research, 16(1)

Published By: SAGE Publishing

URL: https://doi.org/10.1177/11786221221150186

Hydrological Components and Sediment Yield Response to Land Use Land Cover Change in The Ajora-Woybo Watershed of Omo-Gibe Basin, Ethiopia

Air, Soil and Water Research
Volume 16: 1–17

DOI: 10.1177/11786221221150186

Meseret Bekele Toma, Mulugeta Dadi Belete and Mihret Dananto Ulsido

Hawassa University, Hawassa, Ethiopia

ABSTRACT: Understanding how watersheds respond to ecological changes and how LULC alteration affects watershed hydrology is crucial for water and soil resource management. LULC changes in the Ajora-Woybo watershed, Ethiopia, have momentously affected the water and soil resources. The researchers aimed to see how LULC changes affect hydrological components (HCs) and sediment yield (SED) in the watershed, both historically and in the future. The Soil and Water Assessment Tool (SWAT2012) and Partial Least Squares Regression (PLSR) models were used to investigate the contribution of each of the LULC classes to achieve the goal. The findings revealed a continual growth of cultivated land, built-up areas, and bare land, and a retreat of shrub land and forest land during the 2000 to 2020 periods, which is expected to continue in the 2035 and 2050 periods. Changes in LULC that happened over the historical era increased yearly surface runoff (23.5%), water yield (5.7%), and sediment yield (23.5%). On the other hand, the observed modifications have reduced lateral flow (12.8%) and groundwater flow (10.9%). Except for the 2020 LULC period, evapotranspiration decreased during the studied years. The future impacts of LULC states are predicted to increase in line with the historical trend. The PLSR results showed that cultivated land and built-up areas had a positive association with surface runoff and sediment yield, but shrub land and forest land had a negative correlation. This highlights the importance of controlling the LULC change as soon as possible to maintain long-term watershed stability.

KEYWORDS: LULC, SWAT, PLSR, hydrological components, sediment yield

RECEIVED: September 5, 2022. **ACCEPTED:** December 16, 2022.

TYPE: Original Research

CORRESPONDING AUTHOR: Meseret Bekele Toma, Faculty of Biosystems and Water Resources Engineering, Hawassa University, Hawassa P.O.Box 05, Ethiopia. Email: meseretbekelet@gmail.com

Introduction

One of the critical concerns in global change studies has been the impact of natural and man-made variables on land cover change, particularly the transition from vegetation to another LULC (Assfaw, 2020). LULC refers to the bio-physical cover on the Earth's surface and close sub-surfaces that affects water, sediment, and energy flows (Chilagane et al., 2021; Choto & Fetene, 2019). LULC changes are considered one of the most important elements influencing water and soil resources, which are the fundamental hydrological parameters for basin water resource planning and management (Leta et al., 2021). Because of their unavoidable consequences, human activities demand additional consideration when analyzing water and soil losses (Huang & Lo, 2015). The impact of LULC change on HCs such as surface runoff (SURQ), lateral flow (LATQ), groundwater flow (GWQ), and evapotranspiration (ET) in a river basin is a well-studied issue around the world (Abe et al., 2018; Chilagane et al., 2021; Kumar et al., 2018). LULC variations have been studied at various geographical and temporal ranges for their impact on hydrology and soil loss (Assfaw, 2020; Baig et al., 2022; Chaemiso et al., 2021; Choto & Fetene, 2019; Gebremichael, 2021; Wang et al., 2022). Furthermore, evaluations of multiple research papers indicate that LULC modification might modify streamflow, hence altering a basin's hydrological components (HCs) and sediment yield (SED) (Afonso de Oliveira Serrão et al., 2022; Kumar et al., 2018; Negese, 2021).

Anthropogenic causes hastened LULC changes, which affect natural resources in general, and water and soil resources in particular (Negese, 2021). All of these causes contribute to a decline in living circumstances (Munoth & Goyal, 2020). Increased SURQ and decreased GWQ contribute to more extreme weather events, runoff, sedimentation, siltation, and water shortages during the dry season, all of which impede socioeconomic development (Leta et al., 2021). Droughts and floods, which have an impact on hydropower and irrigation production, may become more frequent and stay longer as a result of LULC change (Leta et al., 2021). Deprived LULC management and a lack of proper soil conservation methods are the main threats to watershed management and agricultural productivity (Pandey et al., 2021). As a result, understanding how LULC changes affect water and soil resources is critical for watershed management (Nie et al., 2011).

Although the hydrologic cycle at the watershed level is a complex process impacted by geology, geography, soil conditions, and vegetation, it is also influenced by human actions (e.g. land-use practices, reservoir restrictions, and water transfer projects) (Samie et al., 2019). Also, the hydrology of local watersheds can vary greatly, and water flow patterns are frequently determined by a unique combination of soil, LULC, and elevation variables (Tadesse et al., 2015). River basins are essential for hydrological and environmental improvements because they create consistent streamflow from baseflow and runoff (Teshome et al., 2020). As a result, knowing the impact of LULC change on water and soil resources is critical, particularly in nations whose civilizations rely heavily on rain-fed agriculture (Daramola et al., 2022).

According to Liu, Schmalz et al. (2022), understanding historical LULC changes and their interactions with hydrological processes is critical for better supporting future land-use strategies. Conversely, most scholars do not quantify the future repercussions and contributions of certain LULC classes to diverse hydrological responses (Nie et al., 2011). Understanding in what way different LULC types affect watershed hydrology will extensively advance the liability of LULC dynamics on HCs for water resource management (Woldesenbet et al., 2017). Because external factors that influenced the previous shift in LULC change continue to have an impact on the future direction of LULC change (Schilling et al., 2008). For that reason, a better knowledge of LULC change and watershed hydrology at the watershed scale can help to prevent negative consequences.

In Ethiopia, particularly in the Ajora-Woybo watershed, the impact of the LULC change study on hydrological components, soil erosion, and sedimentation is still not addressed, mainly on the scales that are most important for local actors. According to Stefanidis and Stathis (2018), developing cost-effective watershed management and identifying critical soil erosion-prone areas are necessary for the implementation of appropriate mitigation measures. Soil and water conservation have thus been implemented in the watershed for approximately a decade. Nevertheless, its implementation has been hindered by the absence of site-specific, scientifically calculated soil erosion data and priority criteria. It is also unclear how changes in each LULC class affect the HCs and SED of the watershed. The response to this question will aid in estimating the hydrological implications of each LULC modification, which will be useful in future water resource planning and management.

Diverse models are now utilized to estimate the performance of watersheds under LULC changes on hydrological processes and sediment yield with modest modifications and direct application. The combination of LULC change and HCs modeling provides a valuable framework for assessing the environmental impacts of a watershed LULC change (Shao et al., 2013). Hydrological modeling (HM) is a good way to look into the impact of land use, climate, and soil interactions on natural ecosystems (Scott-Shaw et al., 2020). An HM approach was also employed to evaluate the potential implications of past as well as future LULC on HCs and SED (Abe et al., 2018). SWAT is a popular model among hydrologists because it places a heavy emphasis on the environment and hydrological interactions, making it appropriate for LULC-based water and soil losses (Aragaw et al., 2021; Assfaw, 2020; Kumar et al., 2018). SWAT is a semi-distributed and continuous time-step model based on GIS that allows for speedier implementation of input information across diverse river basins and gives an efficient and cost-effective understanding of the effects of LULC change on water and soil resources (Arnold et al., 2012; Samal & Gedam, 2021). Some of the studies that demonstrated the applicability of SWAT in the study basin (Chaemiso et al., 2021; Choto & Fetene, 2019). Therefore, in this study, an integrated technique of SWAT and the PLSR model was applied to evaluate the situation.

In general, this research assessed the HCs and SED in the Ajora-Woybo watershed, utilizing historical and future LULC change scenarios. Understanding the effects of LULC change is necessary for long-term water resource sustainability, adaptation options, and effective water resource management in the future. Additionally, the study evaluated the localization of erosion-prone sites. Accurate quantitative estimates of soil loss rates are crucial for developing and putting into practice appropriate soil and water conservation policies. This research could also aid policymakers in making more long-term judgments when executing watershed development plans in a particular area.

Material and Methods

Description of the study area

The Omo-Gibe basin in Ethiopia is 79,000 km^2 in area, measuring 550 km in length and 140 km in width. The Ajora-Woybo watershed, located on the eastern edge of the middle Omo-Gibe basin, is one of the basin's principal watersheds. It was chosen as the case study for this investigation. The Ajora-Woybo watershed contains four perennial rivers (Ajancho, Soke, Shapa, and Woybo) that flow downstream to the lower valley and finally form two rivers, Ajora and Woybo, which eventually join the Gibe III dam reservoir (Figure 1). In addition, the rivers are fed by several tiny intermittent tributaries. The watershed is located between latitudes 7°2′0″N and 7°50′0″N and longitudes 37°30″0″E and 38°0″0″E. The climate of the Ajora-Woybo watershed ranges from a hot arid environment in the floodplain to a tropical humid climate in the highlands, which encompass the extreme north and northeastern parts of the watershed. The climate is tropical and subhumid. Weather patterns and agricultural production practices vary by zone. Annual precipitation varies substantially from north to south, ranging from approximately 1,900 mm in the north to less than 300 mm in the south. Furthermore, the watershed rainfall regime is bimodal. The mean annual temperature ranges from 16°C in the northern highlands to more than 29°C in the southern lowlands.

Data

The SWAT model requires the following input data, as stated in Table 1.

DEM: It was entered into the SWAT model to determine the watershed, extract topography or slope data, and evaluate terrain drainage patterns. A 20 m × 20 m DEM was used for this study.

LULC: The historical LULC images were obtained from Landsat images (4–5 TM, 7 ETM+ and 8 OLI) and classified using supervised classification in Earth Resource Data Analysis System (ERDAS) imagine 2015 model. Based on

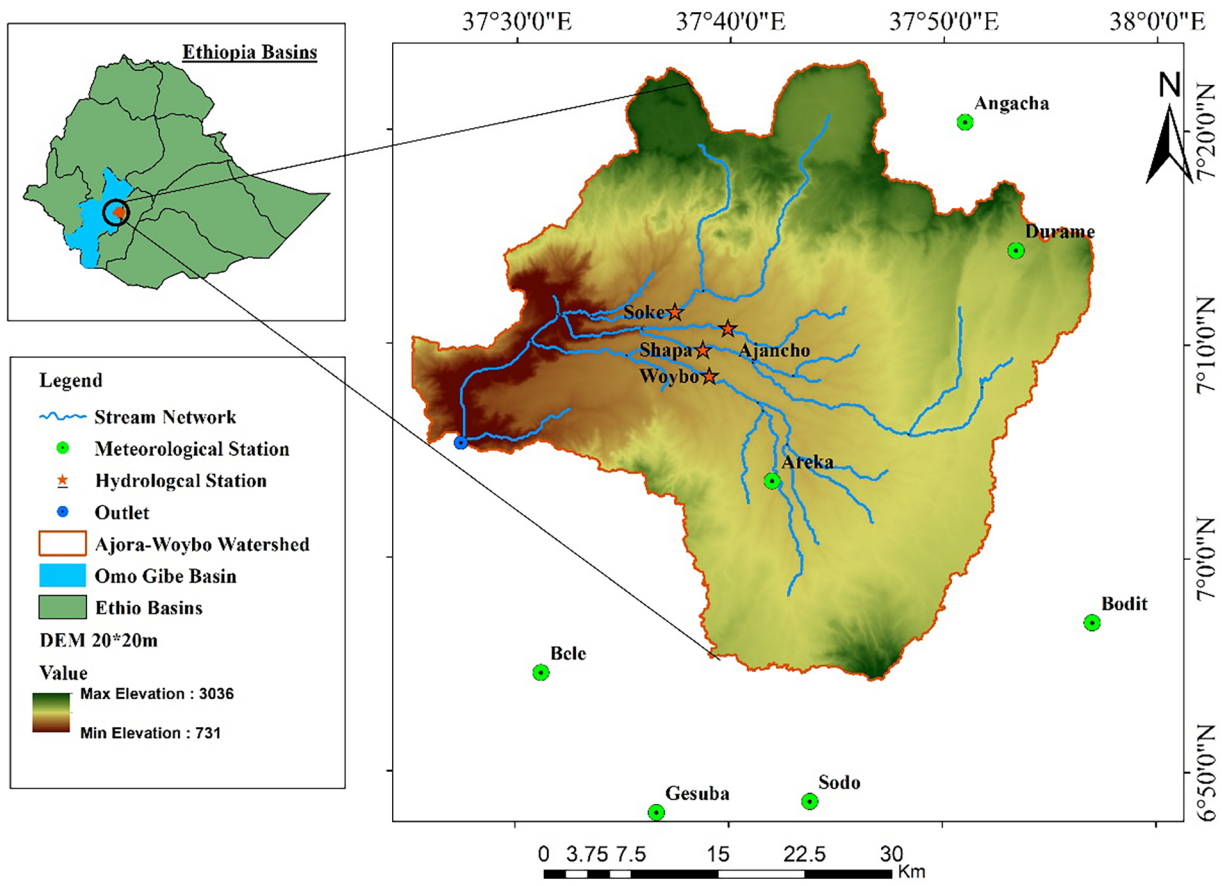

Figure 1. Study area map.

Table 1. Data for the Model.

DATA TYPE	FORMAT	DATA DETAILS	SOURCE	PERIOD
DEM	Raster	20 × 20 m	USGS	2020
LULC	Raster	30 × 30 m	USGS and predicted	2000, 2010, 2020, 2035 and 2050
Soil types	Raster	1:50,000	MoWE	2020
Daily climate	Text	Gaging stations	NMA	1990 to 2020
Daily flow and SED	Text	Gaging stations	MoWE	1990 to 2015

Note. DEM = Digital Elevation Model; USGS = US Geological Survey; MoWE = Ministry of Water and Energy; NMA = National Meteorological Agency, Ethiopia.

classified historical satellite photographs, the future LULC was anticipated. The Land Change Modeler included in TerrSet model version 18.31 was used for this. As a result, the classified historical LULC data for three time periods (2000, 2010, and 2020) as well as the two forecasted time periods (2035 and 2050) were displayed in detail by Toma et al. (2022) and utilized in this study (Figure 2). The classified LULC classes of the Ajora-Woybo watershed are cultivated land (CL), built-up areas (BUA), shrub land (SHL), forest land (FL), bare land (BL), and water body (WB) (Toma et al., 2022).

Soil: Physicochemical and hydrological parameters, were determined for each soil polygon. Dystric nitisols (45.8%), Pellic vertisols (38.5%), Chromic luvisols (10.5%), Eutric cambisols (4.6%) and Leptosols (0.4%) are the major soils in the watershed (Figure 3).

Description and set up of SWAT model

The model was developed over a 30-year period by the US Section of Agricultural Research Service. It is used to simulate the impact of LULC difference on HCs and SED over lengthy time periods with changing LULC, climate, soils, and management (Arnold et al., 2012). For this investigation, a SWAT2012 interface compatible with ArcGIS version 10.3 was used.

The delineation of the watershed is the first stage in creating SWAT model input. Prior to dealing with raster input data such

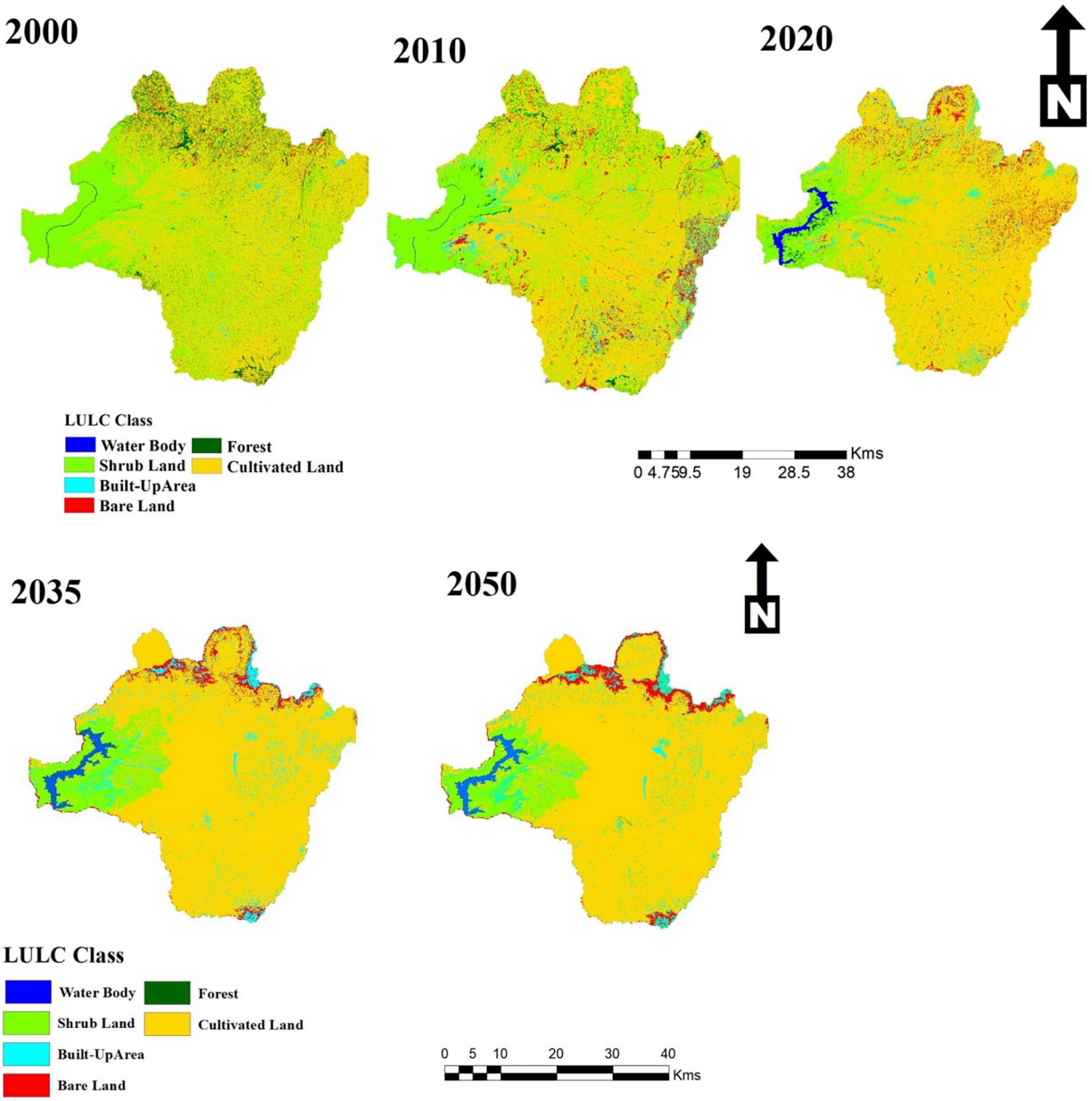

Figure 2. Classified and predicted LULC map in the Ajora-Woybo watershed.

as the DEM, LULC, and soil maps, which were all projected into Ethiopia's projection parameters (UTM Zone 37N). All of these physical parameters were overlaid for hydrological response units (HRUs) definition after reclassifying LULC, soil, and slope in the SWAT database. The lowest area threshold values for land use, soil, and slope were defined as 5%, 5%, and 5%, respectively, and 25 sub-basins and 192 HRUs were identified, representing inimitable amalgamations of land use, soil type, and slope.

The simulation process is allocated into two parts: (1) the land phase and (2) the routing phase, which are used to simulate the HCs and SED of the Ajora-Woybo watershed. The first phase takes into account HCs such as SURQ, LATQ, GWQ, water yield (WTYD), and ET. The watershed channel network is used to track the flow of water and SED in the second phase. The simulation of the model is established on the water balance equation (Arnold et al., 2012; Neitsch et al., 2005).

$$SW_T = SW_O + \sum_{i=1}^{n}\left(R_{day} - Q_{surf} - E_a - W_{seep} - Q_{gw}\right) \quad (1)$$

Where, SW_T is the last soil water satisfied, SW_O is the early water satisfied, n is the time, R_{day} is the amount of rainfall, Q_{surf} is the volume of SURQ, E_a is the extent of E_T, W_{seep} is the extent of water arriving the vadose zone, and Q_{gw} is the degree of return flow. Except for n, which is measured in days, other physiognomies are measured in millimeters.

The Soil Conservation Service curve number (SCS-CN) approach is used to estimate SURQ (Neitsch et al., 2005). The SCS-CN equation is:

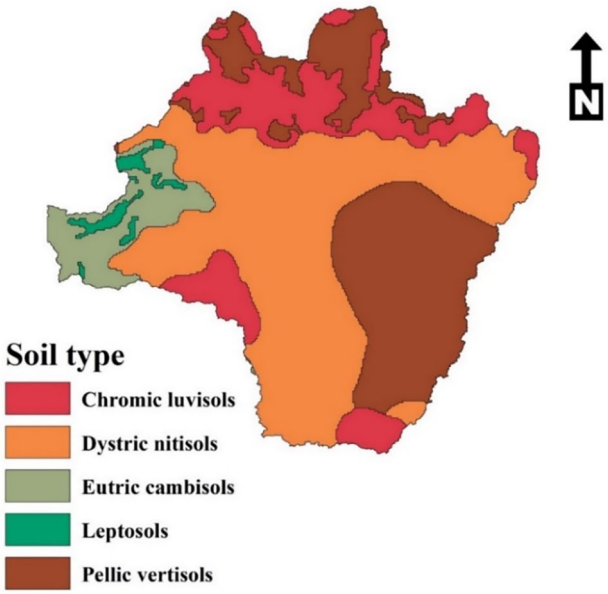

Figure 3. Soil types in the Ajora-Woybo watershed.

$$Q_{surf} = \frac{\left(R_{day} - 0.2S\right)^2}{\left(R_{day} + 0.8S\right)} \quad (2)$$

Where, Q_{surf} is the total SURQ, R_{day} is the daily rainfall depth, S is the retention. The equation that defines the S limit was:

$$S = 25.4\left(\frac{1000}{CN} - 10\right) \quad (3)$$

Groundwater flow: It is calculated using the hydraulic conductivity, the aloofness from the sub basin to the main channel, and the water table height.

$$aqsh,i = aqsh,_{i-1} + Wrchrg + Qgw - Wdeep - Wpump,sh \quad (4)$$

Where, $aqsh,i$ is the water kept in the aquifer on day i, $aqsh,_{i-1}$ is the water kept in the aquifer on day i_1, W_{rchrg} is the recharge entering the aquifer, Q_{gw} is the GWQ, W_{deep} is the deep percolating water, and W_{pump}, sh is the water extracted from the aquifer. All parameters are in mm.

ET: Evaporation and transpiration are calculated separately: evaporation is assessed by means of a linear function of potential evapotranspiration and leaf area index, while transpiration is assessed by means of an exponential function of soil depth and water content. In this study, the Penman–Monteith technique was used to compute ET.

WTYD: The residual water yield to the stream channel was calculated by adding SURQ, LATQ, GWQ, and transmission loss (Tloss).

SED: The SED for individual sub-basin is computed, and the total SED is directed to the watershed outlet. The Modified Universal Soil Loss Equation (MUSLE) was applied to calculate SED at an HRU level (MUSLE). Since SURQ is a result of precursor moisture conditions as well as rainfall drive, this strategy enhanced sediment output prediction (Chimdessa et al., 2018; Neitsch et al., 2005).

$$Sed = 11.8 * \left(Q_{surf} * q_{peak} * area_{bru}\right)^{0.56} * K * C * P * LS * CFRG \quad (5)$$

Where, Sed is the SED (metric tons/day), Q_{surf} is the SURQ (mm/ha), q_{peak} is the peak runoff (m^3/s), $area_{hru}$ is the area (ha), K is the soil erodibility factor, C is the cover factor (dimensionless), P is the USLE conservation practice factor (dimensionless), LS is the topographic factor (dimensionless) and CFRG is the course fragment factor (dimensionless).

Weather Generator (WGEN): All-climate variables must have daily values derived from measured data, as well as values derived from monthly average data over several years. Nonetheless, there is a scarcity of complete and representative long-term climatic data in the study area. As a result, the weather generator answers this issue by producing data from observed data (Sodo station). The weather generator produces precipitation (as PCP), maximum and minimum temperatures (as TMP), solar radiation (as SLR), relative humidity (as HMD) and wind speed (as WND) individually.

Sensitivity analysis

During model simulation, a model sensitive analysis is required to find the most sensitive parameters and decrease parameter joblessness (Pandey et al., 2021). The sensitivity of each parameter was determined using a global sensitivity analysis. The most sensitive parameters that greatly influence the flow and sedimentation processes were found individually using the sensitivity analysis. The parameters were ranked using the most recent iterations of t-stat and p-value. As a result, a higher absolute value t-test implies greater sensitivity, while a p-value of zero shows greater significance. Based on the literature and the weight of parameters, sixteen and nine parameters for flow and sediment, respectively, were examined and tested for sensitivity analysis (Tables 2 and 3).

Calibration and validation

Monthly flow (1990–2015) and suspended sediment load (1990–2015) at Woybo and Soke River gaging stations were utilized independently to calibrate and validate the model. To do this, simulations from 1990 to 1992 were utilized for warm-up, 1993 to 1997, 2001 to 2006, and 2011 to 2013 for calibration, and 1998 to 2000, 2007 to 2010, and 2014 to 2015 for validation. The method in this algorithm attempts to capture the majority of the measured data inside the 95% prediction uncertainty (95PPU) band. Validation was performed after calibration with no further changes in the values of the sensitive calibration parameters. The Sequential Uncertainty Fitting

Table 2. Sensitive Parameters for Flow.

PARAMETERS	DESCRIPTIONS
R__CN2.mgt	Initial SCS curve number
R__CH_K2.rte	Effective hydraulic conductivity (mm/h)
R__SOL_Z.sol	Depth from the soil surface to the bottom of layer
V__GWQMN.gw	Depth of water for return flow (mm)
R__SURLAG.bsn	Surface runoff lag coefficient
R__ESCO.bsn	Soil evaporation compensation factor.
R__GW_REVAP.gw	Groundwater "revap" coefficient.
R__SOL_ALB.sol	Moist soil albedo
R__GW_SPYLD.gw	Specific yield of the shallow aquifer
R__SOL_AWC.sol	Available water capacity of the soil layer (water/mm soil)
R__SOL_BD.sol	Moist bulk density
R__CH_N2.rte	Main channel (Manning)
V__GW_DELAY.gw	Groundwater delay time (d)
R__REVAPMN.gw	Depth of water for evaporation (mm)
R__SOL_K.sol	Saturated hydraulic conductivity (mm/h)
V__ALPHA_BF.gw	Baseflow alpha (d)

(SUFI-2) approach, which typifies uncertainty, was used in SWAT-CUP2019.

Model competence

It was evaluated by comparing the model simulation results in relation to the observed data (Moriasi et al., 2007). Most HM are evaluated by comparing simulated and measured hydrographs using coefficients of determination (R^2), Nash-Sutcliffe efficiency (NSE) and percent bias (PBIAS) (Table 4).

$$R^2 = \frac{\sum\left(Xi - Xav\right) * \sum\left(Yi - Yav\right)}{\sum\sqrt{\left(Xi - Xav\right)^2} * \sum\sqrt{\left(Yi - Yav\right)^2}} \quad (6)$$

$$ENS = 1 - \frac{\sum\left(Xi - Yi\right)^2}{\sum\left(Xi - Xav\right)^2} \quad (7)$$

$$PBIAS = \frac{\sum_{i=1}^{n}\left(Xi - Yi\right) * 100}{\sum_{i=1}^{n}\left(Xi\right)} \quad (8)$$

Where, Xi = measured flow (m^3/s), Yi = simulated flow (m^3/s), Xav = average measured flow (m^3/s) and Yav is average simulated flow (m^3/s).

Table 3. Sensitive Parameters for Sediment Yield.

PARAMETERS	DESCRIPTIONS
R__USLE_P.mgt	USLE support practice factor
R__SOL_K.sol	Saturated hydraulic conductivity (mm/h)
R__CH_COV1.rte	Channel erodibility factor
R__CH_EQN.rte	Sediment routing method
R__USLE_K.sol	Soil conductivity (mm/h)
R__SPCON.bsn	The linear factor for channel sediment routing
R__SPEXP.bsn	The exponential factor for sediment routing
R__USLE_C.plant.dat	USLE cover factor
R__CH_COV2.rte	Channel cover factor

Sediment rating curve (SRC)

It is a frequently used method for assessing the suspended sediment load (SSL) carried by a river by establishing a link between river discharge and sediment load (SL) (Assfaw, 2020). Because SSL records lack a continuous time step, the SRC for this investigation was generated from empirical relationships between river discharges and related SSL (Arnold et al., 2012). The overall correlation of the SRC includes SL (ton/day), discharge (cumecs) and constants (a and b).

$$Q_s = a * Q^b \quad (9)$$

The initial task was to convert the measured SSL (mg/l) data at Woybo and Soke stations into SL (ton/day) using:

$$S = 0.0864 * Q * C \quad (10)$$

Where, S is the SL (ton/day), Q is the discharge (m^3/s), C is the SSL (mg/l), and 0.0864 is the conversion factor. Following the calculation of the SL, the next step was to establish a relationship between the continuous observed discharge and SL in a daily time step (Assfaw, 2020) (Figure 4).

Scenario development

After determining the most sensitive values for the specified parameters, the SURQ and SED were simulated by altering the LULC map under constant DEM, soil, and climate conditions. LULC maps from the years 2000, 2010, and 2020 were utilized for historical scenarios, while LULC maps from the years 2035 and 2050 were used for future scenarios.

Partial least square regression

The PLSR approach is a multivariate statistical technique that combines multiple regressions and principal component

Table 4. Model Efficiency Scores by Moriasi et al. (2007).

PERFORMANCE RATING	R^2	NSE	PBIAS (%)	
			STREAM FLOW	SEDIMENT
Very good	$0.75 < R^2 < 1.00$	$0.75 < NSE < 1.00$	PBIAS $\leq \pm 10$	PBIAS $\leq \pm 15$
Good	$0.65 < R^2 < 0.75$	$0.65 < NSE < 0.75$	$\pm 10 \leq$ PBIAS $\leq \pm 15$	$\pm 15 \leq$ PBIAS $\leq \pm 30$
Satisfactory	$0.50 < R^2 < 0.65$	$0.50 < NSE < 0.65$	$\pm 15 \leq$ PBIAS $\leq \pm 25$	$\pm 30 \leq$ PBIAS $\leq \pm 55$
Unsatisfactory	$R^2 < 0.50$	$NSE < 0.50$	PBIAS $\geq \pm 25$	PBIAS $\geq \pm 55$

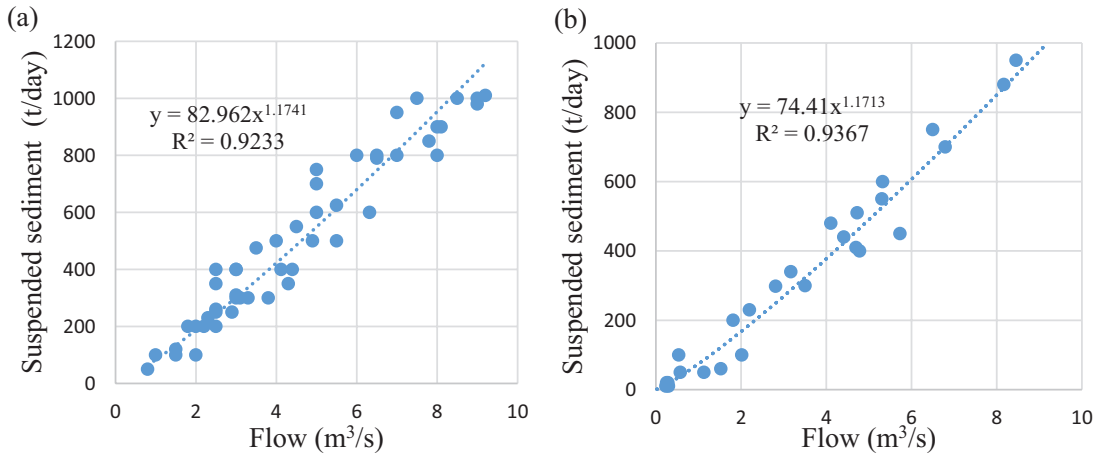

Figure 4. Sediment rating curve of Woybo (a) and Soke (b) river gaging stations.

analysis (Abdi, 2010). It uses a set of predictors to foresee a set of dependent variables. The PLSR model has recently been employed for a variety of hydrological applications, including investigating the effects of changes in specific LULC classes on watershed hydrology at the sub-basin level at a 95% significant level (Gashaw et al., 2018; Nie et al., 2011; Twisa et al., 2020; Woldesenbet et al., 2017). As a result, the PLSR model is beneficial in determining the impact of particular factors (Gashaw et al., 2018; Woldesenbet et al., 2017). The model explains the correlation between a response and a set of predictor variables in such a way that:

$$z = a + x_1 y_1 + x_2 y_2 + x_3 y_3, \ldots, + x_n y_n \quad (11)$$

Where, a and x are the regression coefficients generated from the data, that is, the intercept and variables (1 through n). As a result, it is easy to figure out which LULC types interact the most with the HCs and SED. Annual HCs and SED were employed as dependent variables in PLSR in this study, while individual LULC classes were used as independent variables. The variable importance of projection (VIP) was also utilized to determine the degree of correlation between independent and dependent variables (Aragaw et al., 2021). The importance of the LULC classes for the dependent variables is better explained by predictors with higher VIP values. In general, the scientific community considers a VIP value of 0.8 to be the minimum acceptable value (Abdi, 2010; Gashaw et al., 2018). The changes in dependent and independent variables were considered using LULC maps between 2020 and 2000 for this study.

Identifying places that are prone to erosion

The simulated result of annual average SED mapping was performed after utilizing the calibrated and validated SWAT model. Following that, significant sub-basins prone to soil erosion were identified and selected based on the simulated results for the current (2020LULC) timeframe. The Ajora-Woybo watershed was divided into low, moderate, high, very high, severe, and very severe risk areas, with 0–10 $t\,ha^{-1}y^{-1}$, 10–20 $t\,ha^{-1}y^{-1}$, 20–30 $t\,ha^{-1}y^{-1}$, 30–50 $t\,ha^{-1}y^{-1}$, 50–75 $t\,ha^{-1}y^{-1}$, and >75 $t\,ha^{-1}y^{-1}$, respectively, to better understand the prioritization and classification of SED severity. The soil loss ranks were established based on Ethiopian study findings (Assfaw, 2020; Chaemiso et al., 2021; Chimdessa et al., 2018; Dibaba et al., 2021).

Results and Discussions

Land use land cover change

Figure 5 depicts the LULC stages of the Ajora-Woybo watershed between the years 2000 and 2050. The most substantial changes occurred in six LULC classes, according to a comparison of LULC maps for the years 2000, 2010, 2020, 2035, and

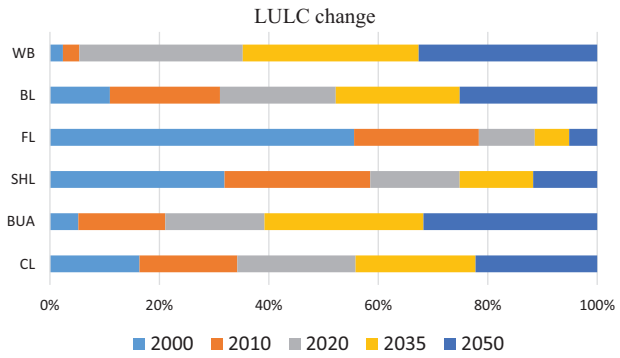

Figure 5. Historical and future LULC dynamics in the Ajora-Woybo watershed.

2050. The assessment of LULC change shows that SHL and FL have been decreasing. However, high increasing rate of CL, BUA, and BL. Similarly, an increase in WB occurred from 2020 to 2050. It is clear from the results that modifications occurred in all LULC classes (Toma et al., 2022). Details on the historical and prospective LULC change analyses, as well as the key causes of LULC change in the Ajora-Woybo watershed, were conducted according to (Toma et al., 2022).

Sensitivity analysis

The greatest influential sensitive parameters for flow and SED were discovered and prioritized according to their sensitivity using the t-stat and the *p*-value at Woybo and Soke gaging stations in this study (Tables 5 and 6). The sensitivity analysis revealed that the parameters played a significant role in affecting stream flow and SED in the Ajora-Woybo watershed. These variables were also mentioned as being important in the Omo-Gibe basin (Chaemiso et al., 2021; Choto & Fetene, 2019), though the rank and fitted value differ. As a consequence, the first 13 flow parameters and the first six SED parameters were used to calibrate and validate the model.

Calibration and validation

For both the calibration and validation periods, monthly scales for the Woybo and Soke gage stations were verified (Table 7 and Figures 6 and 7). Based on the recommendation standards delivered by (Moriasi et al., 2007), the overall SWAT model performance for the research region was judged to be good to very good throughout both the calibration and validation periods. The R^2, ENS, and PBIAS values for monthly flow rate and sediment yield imply the model predictive capacity, and it is appropriate to estimate the HCs and SED owing to LULC changes in the Ajora-Woybo watershed. Similar model efficiency perfections were also recorded during the calibration and validation periods by Chaemiso et al. (2021) and Choto and Fetene (2019). Following that, the information can be used

Table 5. Flow Sensitive Parameters.

PARAMETERS	*T*-STAT	*P*-VALUE	RANK	FITTED VALUE		MIN	MAX
				WOYBO	SOKE		
CN2	21.1	.00	1	−0.03	−0.02	−0.20	0.20
CH_K2	−0.92	.53	13	217.49	223	−0.01	500
SOL_Z	−0.66	.78	16	1312.5	1310	0.0	3500
GWQMN	−1.11	.43	12	1.99	1.9	0.0	2
SURLAG	0.75	.68	15	9.98	10.2	0.05	24
ESCO	13.54	.00	2	0.65	0.68	0.0	1
GW_REVAP	2.51	.04	7	0.17	0.1	0.02	0.2
SOL_ALB	1.47	.04	8	0.02	0.01	0.0	0.25
GW_SPYLD	5.16	.01	4	0.31	0.3	0.0	1
SOL_AWC	1.32	.27	9	0.24	0.25	0.0	1
SOL_BD	2.99	.02	5	2.10	2	0.9	2.5
CH_N2	−1.23	.36	10	0.01	0.01	−0.01	0.3
GW_DELAY	−2.92	.02	6	250.5	246.3	30	450
REVAPMN	−0.87	.60	14	442.5	442.7	0.0	500
SOL_K	−1.17	.40	11	1470.0	1510	0.0	2000
ALPHA_BF	10.4	.00	3	0.87	0.84	0.0	1

Table 6. Sediment Sensitive Parameters.

PARAMETERS	*T*-STAT	*P*-VALUE	RANK	FITTED VALUE		MIN	MAX
				WOYBO	SOKE		
USLE_P	−2.15	.02	3	0.81	0.78	0.0	1.0
SOL_K	−0.99	.04	6	1990	1781	0.00	2000
CH_COV1	1.22	.03	5	0.22	0.30	−0.05	0.6
CH_EQN	−1.36	.02	4	3.30	3.30	0.00	4.0
USLE_K	−0.85	.59	8	0.34	0.41	0.00	0.65
SPCON	0.84	.61	9	0.01	0.001	0.001	0.01
SPEXP	7.4	.00	1	1.42	1.10	1.0	1.5
USLE_C	4.33	.00	2	0.43	0.38	0.01	0.50
CH_COV2	0.87	.55	7	0.65	0.53	−0.001	1.0

Table 7. SWAT Model Performance Evaluation.

LULC	INDEX	WOYBO		SOKE	
2000 LULC	Calibration (1993–1997)	Flow	Sediment	Flow	Sediment
	R^2	0.8	0.75	0.74	0.68
	ENS	0.77	0.71	0.69	0.61
	PBIAS	2.7	7.4	−3.2	−9.3
	Validation (1998–2000)				
	R^2	0.78	0.73	0.78	0.7
	ENS	0.77	0.69	0.76	0.67
	PBIAS	−3.1	−2.2	1.2	−8.1
2010LULC	Calibration (2001–2006)				
	R^2	0.83	0.82	0.79	0.74
	ENS	0.81	0.76	0.74	0.69
	PBIAS	−1.5	−4.1	2.6	3.1
	Validation (2007–2010)				
	R^2	0.81	0.71	0.78	0.73
	ENS	0.8	0.7	0.75	0.69
	PBIAS	1.2	6.6	−0.9	5.7
2020 LULC	Calibration (2011–2013)				
	R^2	0.83	0.81	0.82	0.81
	ENS	0.81	0.72	0.76	0.75
	PBIAS	−4.2	5.8	0.9	6.2
	Validation (2014–2015)				
	R^2	0.74	0.71	0.72	0.73
	ENS	0.7	0.68	0.7	0.69
	PBIAS	0.9	−5.6	1.7	8.7

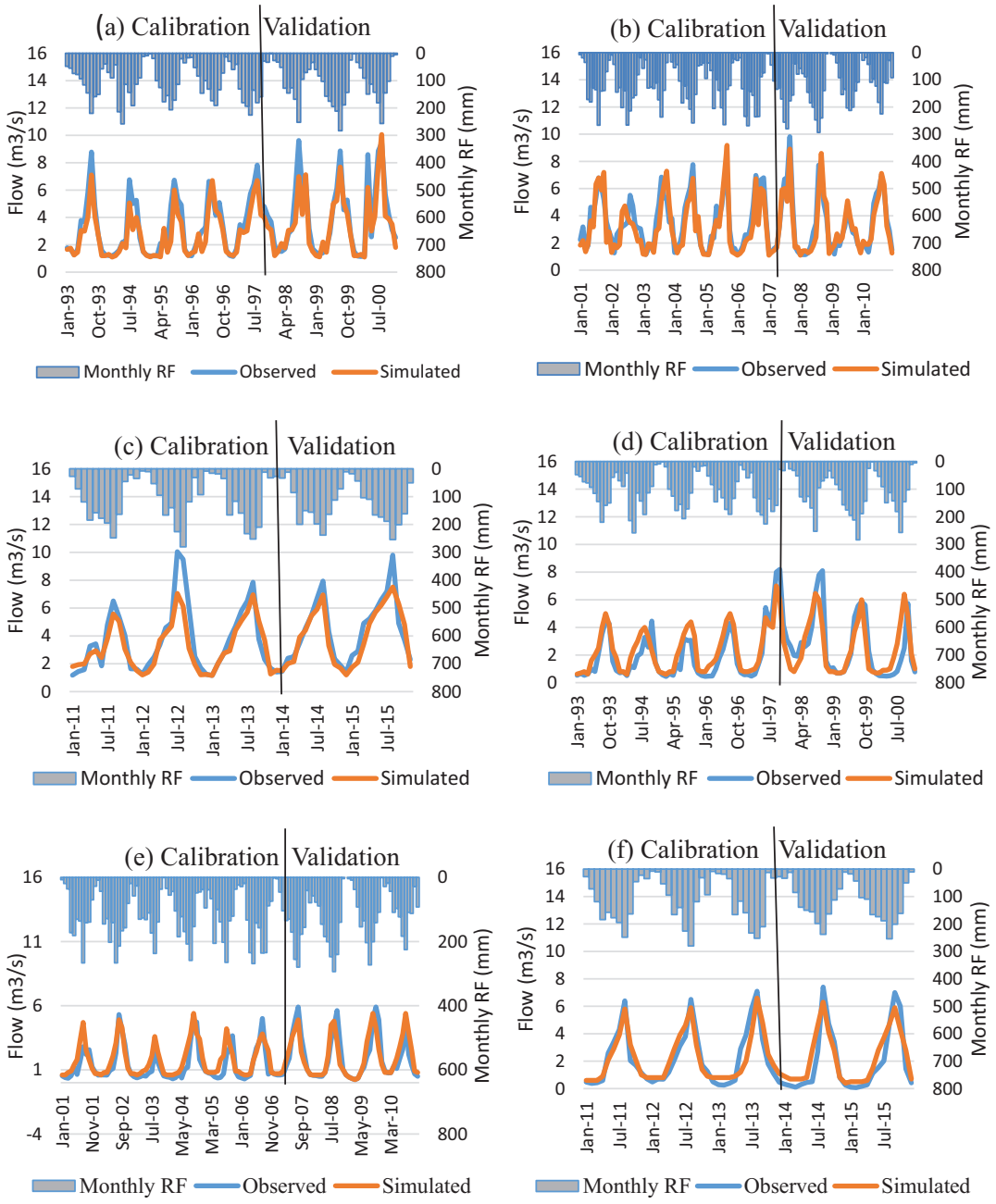

Figure 6. Flow calibration and validation for Woybo (a–c) and Soke (d–f) stations under 2000, 2010, and 2020 LULC, respectively.

to identify and designate sub-basin HCs and important sediment source locations.

Response of HCs and SED to LULC change

Based on the simulation results, HCs and SED responses to LULC changes were examined on a seasonal basis, namely the main rainy season, also known as kiremt (June–September), the small rainy season, also known as Belg (February–May), and the dry season, also known as Bega (October–January).

Seasonal analysis shows (Figures 8 and 9), during the main rainy season (June-September), SURQ for the 2000, 2010, 2020, 2035 and 2050 LULC was 142.2, 171.2, 204.2, 208.9, and 218.9 mm, while the WTYD was 264.2, 275.8, 288.3, 295.3, and 306.3 mm, respectively. During the same season, GWQ was 142.9, 138.9, 133.7, 130.1, and 124.1 mm, while the ET was 91.4, 95.2, 96.2, 96.8, and 97.7 mm. Additionally, in the same season, SED was 17.2, 19.4, 23.5, 25.9, and 28.2 t/ha, respectively. During the small rainy season (February-May), SURQ for the 2000, 2010, 2020, 2035 and 2050 LULC was 104.5, 116.6, 128.4, 130.7, and 131.6 mm, while the WTYD was 132.1, 137.7, 142.4, 144.5, and 145.8 mm, respectively. During the same season, GWQ was 94.8, 78.3, 73.1, 69.5, and 63.4 mm, while the ET was 84.9, 86.4, 88.5, 89.1, and 89.9 mm. Additionally, in the same season, SED was 9.3, 10.1, 11.7, 12.5, and 13.5 t/ha. During the dry season (October-January), SURQ for the 2000, 2010, 2020, 2035 and 2050 LULC was

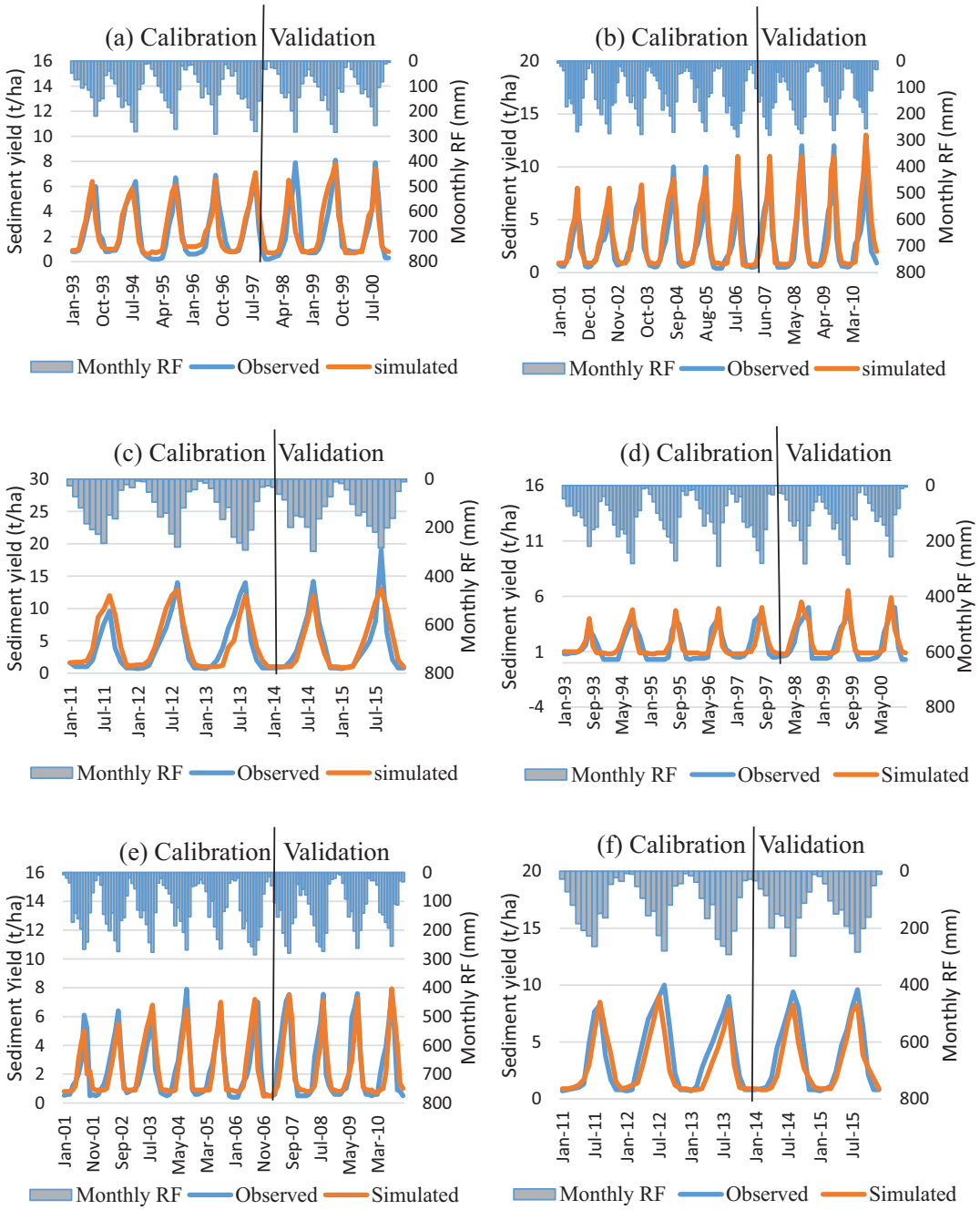

Figure 7. Sediment yield calibration and validation for Woybo (a–c) and Soke (d–f) stations under 2000, 2010, and 2020 LULC, respectively.

105.4, 103.4, 102, 100.8, and 98.1 mm, while the WTYD was 156, 155.2, 151.8, 147.8, and 142.8 mm, respectively. During the same season, GWQ was 86.1, 85.1, 81.7, 78.8, and 75 mm, while the ET was 67.2, 65.8, 64.1, 63.3, 62.8, and 61.2 mm. Additionally, in the same season, SED was 6.3, 5.8, 5.1, 4.3, and 3.75 t/ha.

According to the results, the kiremt season accounts for more than 60% and 45% of SURQ and GWQ for all LULC time periods, respectively, whereas the belg and bega rainy seasons account for less than 40% of SURQ (Figure 8). In addition, the SED rate is the highest in the kiremt season (60%), followed by the belg season (29%) and the bega season (11%). The seasonal results show that due to LULC changes, the SURQ in the watershed increased during the kiremt and belg season and declined during the bega. Due to the increase in agricultural land and other changes in land use during the rainy season, the SURQ of the Ajora-Woybo watershed rises more during the rainy season than during the dry. Similarly, the groundwater component decreased overall across all seasons. This suggests that the LULC alterations have reduced groundwater yield in the watershed. Similarly, changes in lateral flow and evapotranspiration due to LULC variations are inferred on a monthly and seasonal basis (Figure 8). The seasonal results show that ET in the watershed increased during the kiremt and belg seasons and reduced during the bega season. This could be due to soil

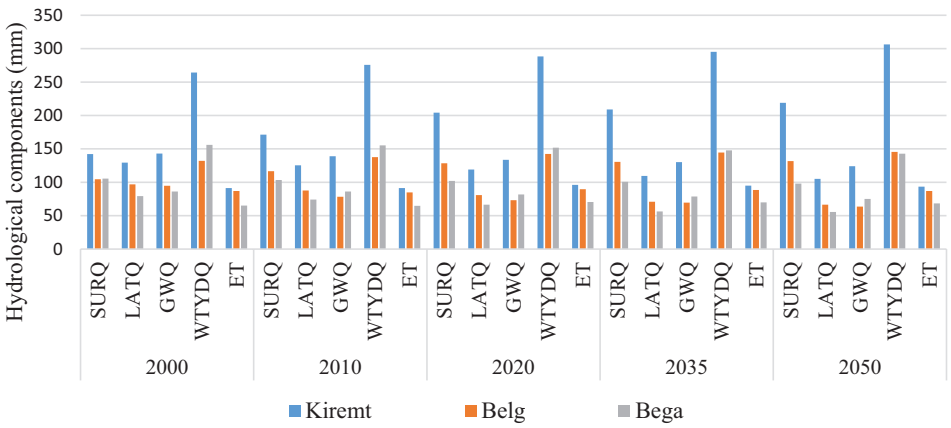

Figure 8. The Ajora-Woybo watershed seasonal HCs.

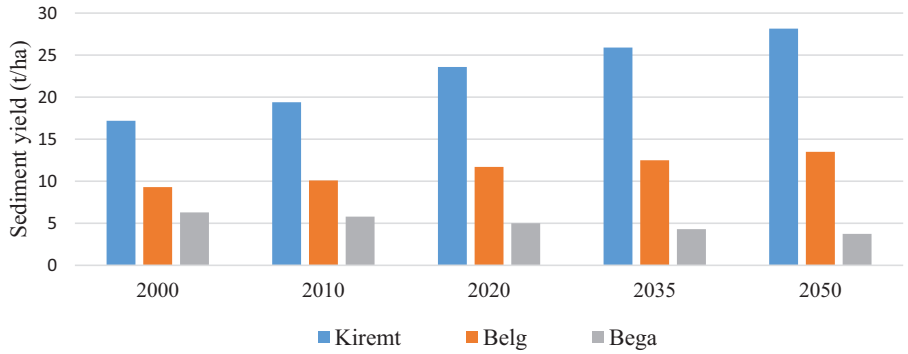

Figure 9. The Ajora-Woybo watershed seasonal SED.

moisture and the condition of the canopy cover during the rainy season.

Heavy rainfall during kiremt season causes large seasonal floods and SURQ over Ethiopia. The reason for this could be that SURQ was more vulnerable in the kiremt than in other seasons. The shift in HCs caused by LULC change lowered runoff during the dry season, which is largely supplied by base flow, and increased runoff during the rainy season, which is mostly supplied by SURQ (Leta et al., 2021; Zhang et al., 2016). According to Woldesenbet et al. (2017), during the dry season, decreased actual ET and GWQ have an opposing effect to streamflow availability. Furthermore, Benegas et al. (2014) proved that improved infiltration is responsible for a decrease in SURQ. High surface runoff caused by LULC changes, as observed in this study, combined with heavy rainfall could result in significant SED during the rainy season. This was also mentioned by Woldesenbet et al. (2017), who stated that increased SURQ during the rainy season has the potential to produce flooding and extreme soil loss. Changes in LULC also have an effect, particularly during the dry season, which has a negative influence on biotic components of ecosystems both inside and beyond the watershed, as well as hydropower generation downstream of the watershed.

The annual variations in the HCs and SED caused by LULC changes revealed effects on the components. Table 8 summarizes the findings, showing that the HCs and SED in the watershed were altered in diverse ways. SURQ, WTYD and SED all increased from the first scenario (2000LULC) to the fifth scenario (2050LULC), whereas LATQ and GWQ dropped. Except for the 2020 LULC period, ET decreased during the studied years. This could be related to the occurrence of a significant body of water from the Gibe III reservoir backflow in the outlet area of the Ajora-Woybo watershed.

Furthermore, SURQ increased by 25.5%, WTYD climbed by 5.7%, and SED increased by 23.5% between 2000 and 2020, whereas LATQ and GWQ declined by 12.8% and 10.9%, respectively. SURQ (by 3.1%), WTYD (by 2.3%), and SED (by 12.8%) increased during the research period (2020–2050), while LATQ (by 14.6%), GWQ (by 8.9%), and ET decreased (by 2.9%). The comparison of SURQ increment and changes in LULCs reveals that the rise in average annual SURQ might be attributable mostly to the growth of cultivated land, built-up areas, and bare land. Besides, the study found that the decrease in LATQ, GWQ and ET are associated with changes in shrub land and forest cover. This was also noted by Nie et al. (2011). They contend that loss of canopy cover reduces percolation and base flow.

For HCs and SED indicators, individual values in 25 subbasins showed a decreasing and growing pattern between 2000

Table 8. Annual Average HCs and SED in the Ajora-Woybo Watershed.

STUDY PERIODS	HYDROLOGICAL COMPONENTS (MM) AND SEDIMENT YIELD (T/HA)					
	SURQ	LATQ	GWQ	WTYD	ET	SED
2000	352.1	305.5	323.8	552.8	243.4	32.8
2010	391	287.2	303.3	569.1	241	35.1
2020	434.7	266.4	288.5	584.5	256.4	40.5
2035	441.4	236.8	278.3	589.3	253.7	42.8
2050	448.3	227.3	262.7	597.9	248.4	45.7
Percent change (%)						
2000–2010	11.0	−6.0	−6.3	2.9	−1.0	7.0
2010–2020	11.2	−7.2	−4.9	2.7	6.4	15.4
2000–2020	23.5	−12.8	−10.9	5.7	5.3	23.5
2020–2035	1.5	−11.1	−3.5	0.8	−1.1	5.7
2035–2050	1.6	−4.0	−5.6	1.5	−2.1	6.8
2020–2050	3.1	−14.7	−8.9	2.3	−3.1	12.8

and 2020. In contrast to HCs, sub-basins with greater growth in agricultural and built-up regions generate more runoff and net water yield. The influence of LULC change on watershed hydrology and sediment output was greater at the sub-basin level than at the watershed level (Figure 10). According to Aragaw et al. (2021), depending on the extent of changes in LULC classes, the influence of LULC class alterations on HCs varies among sub-basins. Choto and Fetene (2019), also observed that sub-basins with a higher share of agriculturally used areas have higher runoff and sediment outputs. As a result, fluctuations in LULC can have a variety of effects on the river flow and SED generating features of any sub-basin. This shows at a smaller scale, the special effects of LULC variations were more pronounced.

The conclusions of this study are reliable with other investigations (Aragaw et al., 2021; Assfaw, 2020; Chaemiso et al., 2021; Chimdessa et al., 2018; Choto & Fetene, 2019; Woldesenbet et al., 2017). They determined that the amount of cultivated land, built-up areas, and bare land is increasing at the expense of vegetation cover (shrub land and forest land), resulting in increased surface runoff and sediment accumulation, as well as decreased GWQ. Many recent articles from around the world have discussed how LULC change influences stream flow and sediment output, as well as the effects of LULC change on water and soil resources (Abe et al., 2018; Chilagane et al., 2021; Daramola et al., 2022).

Individual LULC change effects on HCs and SED

Table 9 shows the regression correlations of the six LULC class with HCs and SED. According to the findings, almost every LULC type had a substantial link with the specific HCs and SED. For instance, cultivated land, built-up areas, and bare land showed positive (significant) correlations with SURQ (0.98), WTYD (0.97), ET (0.91) and SED (0.98), and negative correlations with LATQ (−0.98) and GWQ (−0.94). According to the findings, cultivated land and bare land are the largest contributors to both SURQ and SED, followed by built-up regions, which contribute a lot to SURQ but not much to SED. Shrub land and forest land were shown to contribute to SURQ and SED in opposite directions, with some variance in their contributions to SURQ. Table 10 summarizes the four PLSR models that were built separately.

To differentiate the kin status of predictors, cultivated land, shrub land and forest land (VIP > 1.0) has additional significance in this model. Changes in SURQ and WTYD were shown to be dependent on cultivated land, built-up areas, bare land, and water bodies (on the positive regression coefficient), as well as shrub and forest land (on the negative regression coefficient). The highest VIP values for SURQ and WTYD are obtained for shrub land (VIP = 1.046), followed by cultivated land (VIP = 1.034), and forest land (VIP = 1.024). VIP values for LATQ and GWQ are highest for shrub land (VIP = 1.038), followed by forest land (VIP = 1.036), cultivated land (VIP = 1.023), and bare land (VIP = 1.004). The water body has the greatest VIP value for ET (VIP = 1.306), followed by cultivated land (VIP = 1.206) and shrub land (VIP = 1.172). Cultivated land (VIP = 1.092) has the greatest VIP rating for SED, followed by shrub land (VIP = 1.091), and water body (VIP = 1.051). The weight value in Table 10 demonstrated the relatively low and high impact of LULC classes in influencing HCs and SED of the Ajora-Woybo watershed.

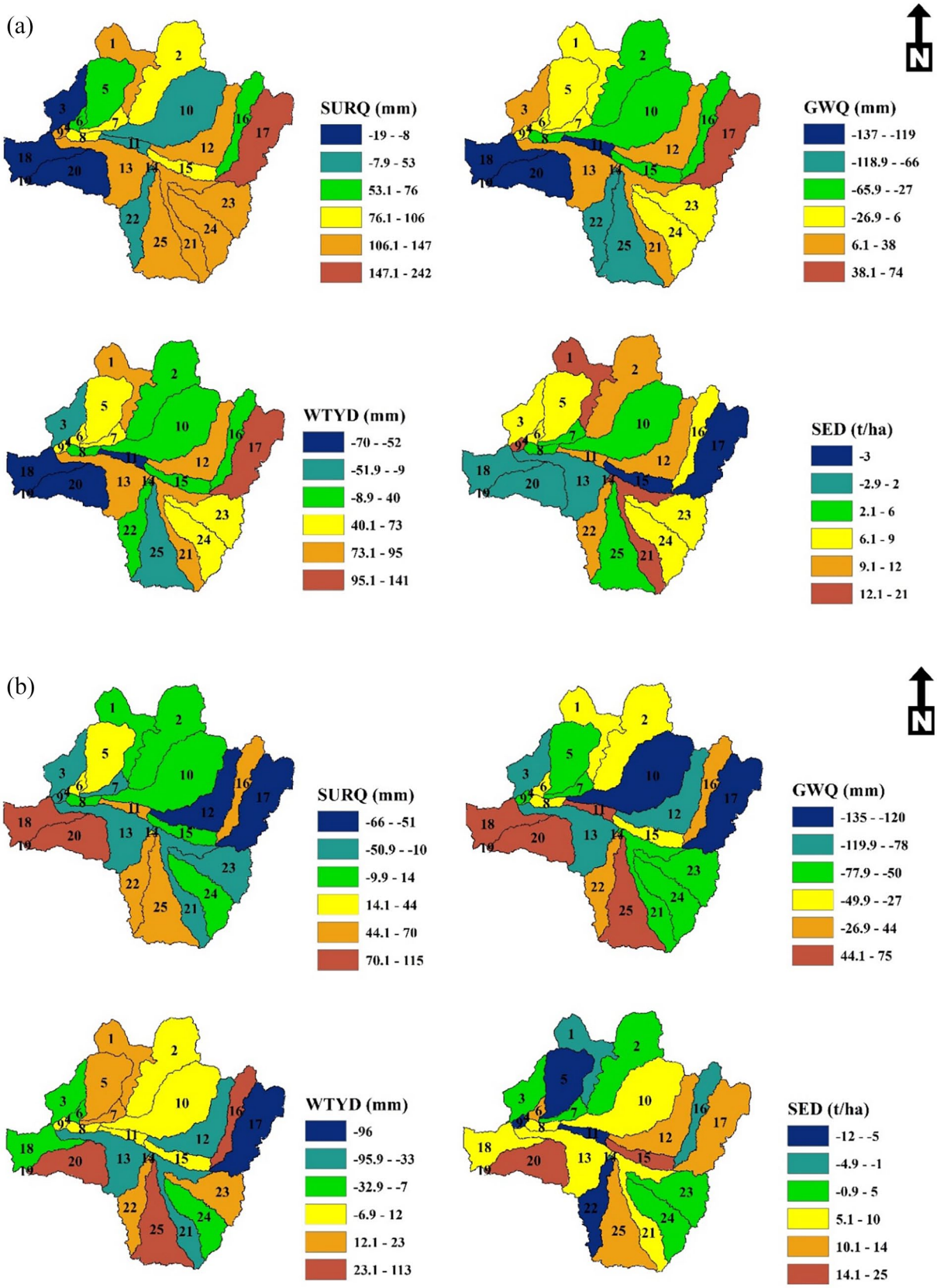

Figure 10. Changes in SURQ, GWQ, WTYD, and SED at the sub-basin level for the years 2000 to 2020 (a) and 2020 to 2050 (b).

Considering separable LULC classes for each HCs and SED, conversion in cultivation land exaggerated SURQ and WTYD positively, but prejudiced LATQ and GWQ negatively (Tables 9 and 10). This suggests that as the Ajora-Woybo watershed's cultivated area expanded, SURQ climbed while LATQ and GWQ decreased. The increased SURQ, coupled

Table 9. PLSR Correlation for LULC Changes (2000–2020) in HCs and SED.

INDEX	CL	BUA	SHL	FL	BL	WB	SURQ	LATQ	GWQ	WY	ET	SED
CL	1.00											
BUA	0.82	1.00										
SHL	−0.96	−0.85	1.00									
FL	−0.88	−0.99	0.91	1.00								
BL	0.78	0.99	−0.82	−0.98	1.00							
WB	0.97	0.65	−0.95	−0.73	0.59	1.00						
SURQ	0.98	0.92	−0.99	−0.96	0.89	0.89	1.00					
LATQ	−0.98	−0.92	0.99	0.96	−0.89	−0.89	−0.87	1.00				
GWQ	−0.94	−0.96	0.96	0.99	−0.94	−0.83	−0.76	0.99	1.00			
WY	0.97	0.94	−0.98	−0.97	0.92	0.87	0.99	−0.98	−0.97	1.00		
ET	0.91	0.51	−0.69	−0.81	0.45	0.99	0.81	−0.81	−0.72	0.77	1.00	
SED	0.98	0.83	−0.97	−0.89	0.79	0.96	0.98	−0.98	−0.95	0.97	0.90	1.00

Table 10. VIP and Weights (W*) of HCs and SED in the Ajora-Woybo Watershed.

INDEX	SURQ, WTYD		LATQ, GWQ		ET		SED	
	VIP	W*	VIP	W*	VIP	W*	VIP	W*
CL	1.034	0.422	1.023	−0.418	1.206	0.492	1.092	0.446
BUA	0.991	0.405	1.004	−0.410	0.608	0.278	0.908	0.371
SHL	1.046	−0.427	1.038	0.424	1.172	−0.478	1.091	−0.446
FL	1.027	−0.419	1.036	0.423	0.801	−0.327	0.969	−0.396
BL	0.962	0.393	0.978	−0.399	0.681	0.246	0.864	0.353
WB	0.935	0.382	0.916	−0.374	1.306	0.533	1.051	0.429

Note. In the PLSR model, the loadings are represented by positive and negative signs.

with a decrease in actual ET due to the expansion of cultivation land and a decline in shrub land and forest land, would result in increased streamflow mainly in the rainy season and decreased in the dry season. Deforestation in the watershed reduced actual ET while increasing surface run-off SURQ and WTYD. Similar to the findings of this study, an escalation in surface runoff, as well as a decrease in groundwater flow, and ET, was seen in the Gidabo basin by Aragaw et al. (2021) and the Andassa watershed by Gashaw et al. (2018), in two watersheds of central America by Benegas et al. (2014), in the Wami basins of Tanzania by Twisa et al. (2020) and the Xunwu watershed of China by Liu, Schmalz et al. (2022).

Identification of hotspot areas in SED

The sub-basin was classified in to different categories of soil erosion categorization based on study experiences in Ethiopia (Assfaw, 2020; Chimdessa et al., 2018; Choto & Fetene, 2019; Megersa et al., 2019). It was assumed to allocate the priority stages of I–VI (Table 11). For present scenarios (2020 LULC), the largest possible SED in each sub-basin was analyzed and plotted, as shown in Figure 11. Sub basins 1 and 2 are falling under very severe erosion classes, while sub-basin 3, 7, 8, 12, 16, and 17 are falling under severe erosion classes. Furthermore, sub-basins 5, 9, 11, 14, 19, 21, and 22 fall under very high erosion classes, while the remaining sub-basins fall under high, moderate and low erosion classes. This graphic depicts how much the watershed is currently vulnerable to erosion as a result of more intensive agricultural activity and urbanization. It is necessary to implement proper best management scenarios in places that are prone to erosion.

Conclusions

This study predicted the potential impacts of LULC change on annual and seasonal HCs and SED distribution, in the Ajora-Woybo watershed of Omo-Gibe River basin, Ethiopia. According

Table 11. Sediment yield (t/ha) and treatment priority order based on the 2020 LULC.

SEDIMENT YIELD (T/HA)	SUB-BASIN	AREA (HA)	AREA (%)	SOIL EROSION CLASS	PRIORITY CLASS
0–11	4, 18	7635.3	4.4	Low	6
11–20	6, 20	10672.4	6.2	Moderate	5
20–30	10, 13, 15, 23, 24, 25	63308.9	36.7	High	4
30–50	5, 9, 11, 14, 19, 21, 22	29192.2	16.9	Very high	3
50–75	3, 7, 8, 12, 16, 17	38901.3	22.6	Severe	2
>75	1, 2	22589.9	13.1	Very severe	1

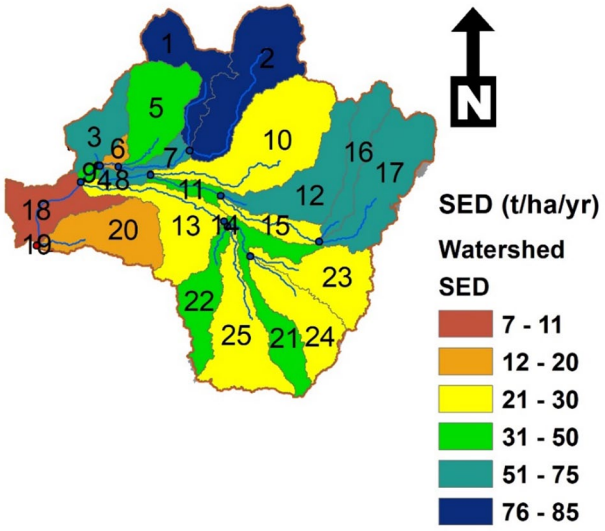

Figure 11. SED (t/ha/yr) in the Ajora-Woybo watershed.

to the model efficiency norms used in this work, the SWAT model was able to predict the HCs and SED processes in the Ajora-Woybo watershed adequately. As a consequence, it was able to simulate changes in watershed HCs and SED in response to various LULC situations. The PLSR model was utilized to determine the relationship between LULC type, HCs, and SED.

The CN2, ESCO, ALPHA_BF, GW_SPYLD, and SOL_BD model parameters have the greatest sensitivity on streamflow, whereas the SPEXP, USLE C, USLE P, and CH_EQN model parameters have the greatest sensitivity on SED. The model runs for different LULC periods show that land use change can induce significant HCs variance and an increase in SED. This is primarily due to land degradation (conversion of shrub land and forest land to cultivated land, built-up areas and bare land). Thus, cultivated land development, urbanization, and exposed land are the most significant contributors to SURQ, WTYD, and SED, and can be regarded as the main environmental stressor affecting HCs and SED in the Ajora-Woybo watershed. A decrease in LATQ and GWQ would immediately reduce recharge to shallow aquifers, and would thus be considered a negative influence on watersheds. Individual changes in cultivated land, built-up areas, shrub land, and forested regions were the most important factors of SURQ and SED at any particular time. Changes in cultivated land, built-up areas, and bare land were shown to correlate favorably with changes in SURQ and SED. However, shrub land and forest land were found to correlate negatively with changes in SURQ and SED. The PLSR model was beneficial in examining the effects of LULC classes on HCs and SED.

These findings are predicted to be relevant in the future for sustainable watershed management in the Ajora-Woybo watershed in particular and the Omo-Gibe basin in general. This research also shows how SWAT-based watershed models can be used to analyze LULC change in a watershed and how they can be simply implemented in similar settings around the world. Still, the outcomes of this study could assist environmental managers in developing long-term watershed based LULC adjustments.

Acknowledgements

We would like to thank, Ministry of Water and Energy, and National Meteorological Agency of Ethiopia, for providing hydrological and meteorological data for the study.

Author Contributions

Conceptualization, M.B.T., M.D.B. and M.D.U.; methodology, M.B.T., M.D.B. and M.D.U; software, M.B.T.; validation, M.B.T., M.D.B. and M.D.U; formal analysis, M.B.T., M.D.B and M.D.U; investigation, M.B.T.; writing—original draft preparation, M.B.T.; writing—review and editing, M.B.T., M.D.B. and M.D.U.; supervision, M.D.B. and M.D.U. All authors have read and agreed to the published version of the manuscript.

Funding

The author(s) received no financial support for the research, authorship, and/or publication of this article.

Declaration of Conflicting Interests

The author(s) declared no potential conflicts of interest with respect to the research, authorship, and/or publication of this article.

Data Availability Statement

Data are available from the corresponding authors upon reasonable request.

REFERENCES

Abdi, H. (2010). Partial least squares regression and projection on latent structure regression (PLS regression). *WIREs Computational Statistics*, 2(1), 97–106. https://doi.org/10.1002/wics.51

Abe, C., Lobo, F., Dibike, Y., Costa, M., Dos Santos, V., & Novo, E. (2018). Modelling the effects of historical and future land cover changes on the hydrology of an Amazonian Basin. *Water*, 10(7), 932. https://doi.org/10.3390/w10070932

Afonso de Oliveira Serrão, E., Silva, M. T., Ferreira, T. R., Paiva de Ataide, L. C., Assis Dos Santos, C., Meiguins de Lima, A. M., de Paulo Rodrigues da Silva, V., de Assis Salviano de Sousa, F., & Cardoso Gomes, D. J. (2022). Impacts of land use and land cover changes on hydrological processes and sediment yield determined using the SWAT model. *International Journal of Sediment Research*, 37(1), 54–69. https://doi.org/10.1016/j.ijsrc.2021.04.002

Aragaw, H. M., Goel, M. K., & Mishra, S. K. (2021). Hydrological responses to human-induced land use/land cover changes in the Gidabo River basin, Ethiopia. *Hydrological Sciences Journal*, 66(4), 640–655. https://doi.org/10.1080/02626667.2021.1890328

Arnold, J. G., Moriasi, D. N., Gassman, P. W., Abbaspour, K. C., White, M. J., Srinivasan, R., Santhi, C., Harmel, R. D., van Griensven, A., Van Liew, M. W., Kannan, N., & Jha, M. K. (2012). SWAT: Model use, calibration, and validation. *Transactions of the ASABE*, 55(4), 1491–1508. https://doi.org/10.13031/2013.42256

Assfaw, A. T. (2020). Modeling Impact of land use dynamics on hydrology and sedimentation of Megech dam watershed, Ethiopia. *Science World Journal*, 2020, 1–20. https://doi.org/10.1155/2020/6530278

Baig, M. F., Mustafa, M. R. U., Baig, I., Takaijudin, H. B., & Zeshan, M. T. (2022). Assessment of land use land cover changes and future predictions using CA-ANN simulation for Selangor, Malaysia. *Water*, 14(3), 402. https://doi.org/10.3390/w14030402

Benegas, L., Ilstedt, U., Roupsard, O., Jones, J., & Malmer, A. (2014). Effects of trees on infiltrability and preferential flow in two contrasting agroecosystems in Central America. *Agriculture Ecosystems & Environment*, 183, 185–196.

Chaemiso, S. E., Kartha, S. A., & Pingale, S. M. (2021). Effect of land use/land cover changes on surface water availability in the Omo-Gibe basin, Ethiopia. *Hydrological Sciences Journal*, 66(13), 1936–1962. https://doi.org/10.1080/02626667.2021.1963442

Chilagane, N. A., Kashaigili, J. J., Mutayoba, E., Lyimo, P., Munishi, P., Tam, C., & Burgess, N. (2021). Impact of land Use and land cover changes on surface runoff and sediment yield in the Little Ruaha River catchment. *Open Journal of Modern Hydrology*, 11(03), 54–74. https://doi.org/10.4236/ojmh.2021.113004

Chimdessa, K., Quraishi, S., Kebede, A., & Alamirew, T. (2018). Effect of land use land cover and climate change on river flow and soil loss in Didessa river basin, south west Blue Nile, Ethiopia. *Hydrology*, 6(1), 2. https://doi.org/10.3390/hydrology6010002

Choto, M., & Fetene, A. (2019). Impacts of land use/land cover change on stream flow and sediment yield of Gojeb watershed, Omo-Gibe basin, Ethiopia. *Remote Sensing Applications Society and Environment*, 14, 84–99. https://doi.org/10.1016/j.rsase.2019.01.003

Daramola, J., Adepehin, E. J., Ekhwan, T. M., Choy, L. K., Mokhtar, J., & Tabiti, T. S. (2022). Impacts of land-use change, associated land-use area and runoff on watershed sediment yield: Implications from the Kaduna Watershed. *Water*, 14(3), 325. https://doi.org/10.3390/w14030325

Dibaba, W. T., Demissie, T. A., & Miegel, K. (2021). Prioritization of sub-watersheds to sediment yield and evaluation of best management practices in highland Ethiopia, Finchaa catchment. *Land*, 10(6), 650. https://doi.org/10.3390/land10060650

Gashaw, T., Tulu, T., Argaw, M., & Worqlul, A. W. (2018). Modeling the hydrological impacts of land use/land cover changes in the Andassa watershed, Blue Nile Basin, Ethiopia. *The Science of the Total Environment, 619-620*, 1394–1408. https://doi.org/10.1016/j.scitotenv.2017.11.191

Gebremichael, A. (2021). Effect of land use land cover change on stream flow and sediment yield in Gibe III watershed, Omo-Gibe Basin, Ethiopia. *Journal of Earth Science & Climatic Chang*, 12(10), 20.

Huang, T., & Lo, K. (2015). Effects of land use change on sediment and water yields in Yang Ming Shan National Park, Taiwan. *Environments*, 2(4), 32–42. https://doi.org/10.3390/environments2010032

Kumar, N., Singh, S. K., Singh, V. G., & Dzwairo, B. (2018). Investigation of impacts of land use/land cover change on water availability of Tons River basin, Madhya Pradesh, India. *Modeling Earth Systems and Environment*, 4(1), 295–310. https://doi.org/10.1007/s40808-018-0425-1

Leta, M. K., Demissie, T. A., & Tränckner, J. (2021). Hydrological responses of watershed to historical and future land use land cover change dynamics of Nashe watershed, Ethiopia. *Water*, 13(17), 2372. https://doi.org/10.3390/w13172372

Liu, G., Schmalz, B., Zhang, Q., Qi, S., Zhang, L., & Liu, S. (2022). Assessing effects of land use and land cover changes on hydrological processes and sediment yield in the Xunwu River watershed, Jiangxi Province, China. *Earth Science Frontiers*, 16, 819–833. https://doi.org/10.1007/s11707-021-0959-9

Megersa, T., Nedaw, D., & Argaw, M. (2019). Combined effect of land use/cover types and slope gradient in sediment and nutrient losses in Chancho and Sorga sub watersheds, East Wollega Zone, Oromia, Ethiopia. *Environmental Systems Research*, 8(1), 24. https://doi.org/10.1186/s40068-019-0151-3

Moriasi, D. N., Arnold, J. G., Liew, M. W., Bingner, R. L., Harmel, R. D., & Veith, T. L. (2007). Model evaluation guidelines for systematic quantification of accuracy in watershed simulations. *Transactions of the ASABE*, 50(3), 885–900. https://doi.org/10.13031/2013.23153

Munoth, P., & Goyal, R. (2020). Impacts of land use land cover change on runoff and sediment yield of upper Tapi river sub-basin, India. *International Journal of River Basin Management*, 18(2), 177–189. https://doi.org/10.1080/15715124.2019.1613413

Negese, A. (2021). Impacts of land use and land cover change on soil erosion and hydrological responses in Ethiopia. *Applied and Environmental Soil Science*, 2021, 1–10. https://doi.org/10.1155/2021/6669438

Neitsch, S. L., Arnold, J. G., Kiniry, J. R., & Williams, J. R. (2005). Soil and water assessment tool theoretical documentation, version 2005. *Grassland, Soil and Water Research Laboratory, Agricultural Research Service*, 76502, 494.

Nie, W., Yuan, Y., Kepner, W., Nash, M. S., Jackson, M., & Erickson, C. (2011). Assessing impacts of Landuse and landcover changes on hydrology for the upper San Pedro watershed. *Hydrology Journal*, 407(1-4), 105–114. https://doi.org/10.1016/j.jhydrol.2011.07.012

Pandey, A., Bishal, K. C., Kalura, P., Chowdary, V. M., Jha, C. S., & Cerdà, A. (2021). A soil water assessment tool (SWAT) modeling approach to prioritize soil conservation management in river basin critical areas coupled with future climate scenario analysis. *Air Soil and Water Research*, 14, 117862212110213. https://doi.org/10.1177/11786221211021395

Samal, D. R., & Gedam, S. (2021). Assessing the impacts of land use and land cover change on water resources in the Upper Bhima river basin, India. *Environmental Challenges*, 5, 100251. https://doi.org/10.1016/j.envc.2021.100251

Samie, M., Ghazavi, R., Vali, A., & Pakparvar, M. (2019). Evaluation of the effect of land use change on runoff using supervised classified satellite data. *Global NEST Journal*. 2, 21. https://doi.org/10.30955/gnj.002631

Schilling, K. E., Jha, M. K., Zhang, Y.-K., Gassman, P. W., & Wolter, C. F. (2008). Impact of land use and land cover change on the water balance of a large agricultural watershed: Historical effects and future directions. *Water Resources Research*, 44(7), https://doi.org/10.1029/2007wr006644

Scott-Shaw, B., Hill, T., & Gillham, J. (2020). Calibration of a modelling approach for sediment yield in a wattle plantation, KwaZulu-Natal, South Africa. *Water SA*, 46. https://doi.org/10.17159/wsa/2020.v46.i2.8232.

Shao, Y., Lunetta, R. S., Macpherson, A. J., Luo, J., & Chen, G. (2013). Assessing sediment yield for selected watersheds in the Laurentian great lakes basin under future agricultural scenarios. *Environmental Management*, 51(1), 59–69. https://doi.org/10.1007/s00267-012-9903-9

Stefanidis, S., & Stathis, D. (2018). Effect of climate change on soil erosion in a mountainous Mediterranean catchment (Central Pindus, Greece). *Water*, 10(10), 1469. https://doi.org/10.3390/w10101469

Tadesse, W., Whitaker, S., Crosson, W., & Wilson, C. (2015). Assessing the impact of land-use land-cover change on stream water and sediment yields at a watershed level using SWAT. *Open Journal of Modern Hydrology*, 05(03), 68–85. https://doi.org/10.4236/ojmh.2015.53007

Teshome, F. T., Bayabil, H. K., Thakural, L. N., & Welidehanna, F. G. (2020). Modeling stream flow using SWAT model in the Bina river basin, India. *Journal of Water Resource and Protection*, 12(03), 203–222. https://doi.org/10.4236/jwarp.2020.123013

Toma, M. B., Belete, M. D., & Ulsido, M. D. (2022). Historical and future dynamics of land use land cover and its drivers in Ajora-Woybo watershed, Omo-Gibe basin, Ethiopia. *Natural Resource Modeling*, 35(3), e12353. https://doi.org/10.1111/nrm.12353

Twisa, S., Kazumba, S., Kurian, M., & Buchroithner, M. F. (2020). Evaluating and predicting the effects of land use changes on hydrology in Wami River Basin, Tanzania. *Hydrology*, 7(1), 17. https://doi.org/10.3390/hydrology7010017

Wang, J., Zhang, J., Xiong, N., Liang, B., Wang, Z., & Cressey, E. (2022). Spatial and temporal variation, simulation and prediction of land use in ecological conservation area of Western Beijing. *Remote Sensing*, 14(6), 1452. https://doi.org/10.3390/rs14061452

Woldesenbet, T. A., Elagib, N. A., Ribbe, L., & Heinrich, J. (2017). Hydrological responses to land use/cover changes in the source region of the Upper Blue Nile Basin, Ethiopia. *The Science of the Total Environment*, 575, 724–741. https://doi.org/10.1016/j.scitotenv.2016.09.124

Zhang, L., Nan, Z., Yu, W., & Ge, Y. (2016). Hydrological responses to land-use change scenarios under constant and changed climatic conditions. *Environmental Management*, 57(2), 412–431. https://doi.org/10.1007/s00267-015-0620-z